SERBIAN JOURNAL OF ELECTRICAL ENGINEERING
Vol. 23, No. 3, October 2026, 465-484
UDC: 004.432.2C++:502.211 **DOI: https://doi.org/10.2298/SJEE2603465C**
Original scientific paper

Hybrid Metaheuristic Method for Vegetation-Rich Outdoor 3D Point Cloud Image Registration

Nebojša Čvorović[1], Ana Gavrovska[1]

Abstract: This paper presents a hybrid metaheuristic point cloud registration procedure combining Differential Evolution (DE) and Particle Swarm Optimization (PSO), referred to as DE-PSO. The method pairs the broad search capabilities of DE with the rapid convergence of PSO, avoiding the local minima traps that degrade standard Iterative Closest Point (ICP) implementations. Vegetation-rich outdoor environments present significant challenges due to dense foliage, irregular geometries, and severe point cloud noise. The proposed DE-PSO strategy addresses these complex scenes, achieving high registration accuracy and avoiding traditional ICP misalignments. Implemented using open-source C++ tools and tested on a custom dataset, the approach yields superior alignment with the lowest root mean square error and fastest execution time compared to standalone configurations. Overall, the method shows the feasibility of combining population-based metaheuristics for complex data, providing a practical tool for outdoor applications where conventional alignment struggles.

Keywords: 3D Spatial Data, Particle Swarm Optimization (PSO), Differential Evolution (DE), Point Cloud Registration, Iterative Closest Point (ICP).

1 Introduction

Point clouds are defined within a three-dimensional (3D) coordinate space, and that space supplies the geometric basis on which physical objects and surroundings are modelled [1, 2]. Depth and mutual spatial relations are retained in such a representation, which is not the case for two-dimensional imagery, so quantities such as shape, scale and spatial arrangement can be measured reliably. The data are nevertheless irregular and frequently corrupted by noise, and this

[1]University of Belgrade, School of Electrical Engineering, Belgrade, Serbia
ncvorovic3@gmail.com, https://orcid.org/0009-0003-4280-412X
anaga777@etf.bg.ac.rs, https://orcid.org/0000-0003-2740-2803
*An earlier version of this paper was presented at the 13th International Conference on Electrical, Electronic and Computing Engineering (IcETRAN), Silver Lake, Serbia, June 2026.

Colour versions of the one or more of the figures in this paper are available online at https://sjee.ftn.kg.ac.rs

©*Creative Common License CC BY-NC-ND*

raises considerable difficulties during processing and interpretation – sparse sampling, occluded regions, outlying points and non-uniform point density being among the most prominent [3 – 5].

Across science, engineering, medicine and, above all, robotics, it is essential to relate two or more 3D representations of the same object to one another in space. The registration task consists of recovering the spatial transformation that brings these representations into the best possible agreement. Once such a mapping has been recovered, the co-aligned models support a broad set of uses: model-based localization, recognition of three-dimensional objects, pose estimation in real time, and the fusion of data from sensors of different modalities. Two families of point cloud registration techniques can be distinguished. One is relying on precise positioning of the navigation system while scanning takes place, the other concerned with accurately merging clouds acquired from differing viewpoints [1, 2].

Aligning multiple spatial perspectives through point cloud registration is critical in computer vision and 3D data processing [2]. Initial results regarding enhanced point cloud registration for 3D outdoor scenes were presented in [1]. Traditionally point cloud registration is anchored by the Iterative Closest Point (ICP) method introduced by Besl and McKay for 3D shapes [6], which was also used in [1]. ICP is a widely used method which assumes that the source and target clouds already lie close to one another. Its behavior is therefore strongly dependent on how the source cloud is initially positioned, and a poor starting pose can drive it quickly into a local optimum. Thus, standard ICP tends to become trapped by local minima when handling complex geometries. To address these limitations, various efficient variants and refinements have been proposed, such as those by Rusinkiewicz and Levoy [3] and Zinsser et al. [4]. To overcome convergence issues in complex scenarios, metaheuristic global optimization techniques are proposed. One of them is Particle Swarm Optimization (PSO) proposed by Kennedy and Eberhart [7]. Another optimization approach is Differential Evolution (DE) by Storn and Price [8]. These techniques have been increasingly integrated into spatial alignment tasks. Researchers have applied these heuristics independently and in hybrid frameworks. For instance, Mezhenin et al. [2] explored hybrid point cloud registration methods, while Zang et al. [5] combined coarse ICP with fine PSO for freeform surface evaluation. Similarly, Tao et al. [9] investigated adaptive differential evolution strategies for point cloud alignment, supported by broader algorithmic applications studied by Karaboğa and Selçuk [10].

An open-source 3D reconstruction pipeline was shown in [11]. Also, advancements in preprocessing, such as the statistical filtering and down-sampling were presented in [12]. More recently, the field has seen a shift toward advanced architecture, including agent-based interaction networks for image-to-

point cloud registration by Cheng et al. [13] and comprehensive deep learning taxonomies by Zhang et al. [14].

This paper addresses the possibilities of using hybrid metaheuristic method for vegetation-rich outdoor 3D point clouds. Because so much depends on how accurate the starting alignment is, the optimization stage largely decides whether an acceptable outcome is reached. The primary contributions of this work are summarized as follows:

- The proposed DE-PSO registration framework integrates the global search capabilities of DE with the rapid convergence of PSO.
- The DE-PSO method demonstrates high robustness, successfully handling vegetation-rich outdoor scenes where standard ICP frequently fails.
- Point cloud data that specifically focus on vegetation outdoor scenes is acquired for the purpose of analysis.
- Comparative evaluation against standalone techniques confirms that the proposed approach achieves the lowest error rates alongside enhanced execution speed.

The rest of this paper is organized as follows: once the fundamentals of 3D registration together with the motivation for and the relevance of the subject have been laid out, Section 2 describes the PSO and DE metaheuristics. Section 3 sets out the configuration adopted for the simulation and indicates how several of the difficulties encountered were resolved. An objective assessment of the outcomes, including a noise-robustness analysis, along with the benefits offered by the proposed registration scheme, is given in Section 4. Section 5 closes the paper with conclusions on the study and on directions for further refinement.

2 Registration and Optimization Algorithms

2.1 Point cloud image registration and Iterative Closest Point (ICP) alignment

A point cloud is a massive collection of spatial data points defined by 3D Cartesian coordinates, often augmented with additional attributes such as color or time. Because individual scans capture only the surfaces exposed to a particular viewpoint, they inherently suffer from occlusions, blind spots, and partial perspectives. Point cloud registration bridges this gap by merging multiple overlapping datasets into a unified global coordinate framework.

Fig. 1 outlines a typical registration pipeline; whose stages are common to most modern point cloud registration approaches. Its inputs are the source and target clouds, which have usually been recorded from dissimilar viewing angles. Preprocessing comes first and serves to suppress the noise carried by the raw sensor measurements. The quality of this step directly affects all subsequent stages, since residual noise propagates into feature computation and matching.

Geometric features are then computed and examined so that the two representations can be related [15]. With features available, a correspondence estimation step determines which points in the source set match points in the target set. A rough, or coarse, registration follows and places the clouds in approximately the right relative position and orientation [16]. Fine alignment is obtained last, through ICP [6]. Beginning from an initial guess of the rigid-body transformation linking the source and target meshes, ICP repeatedly re-establishes correspondences and drives down the alignment error until the registration has been refined.

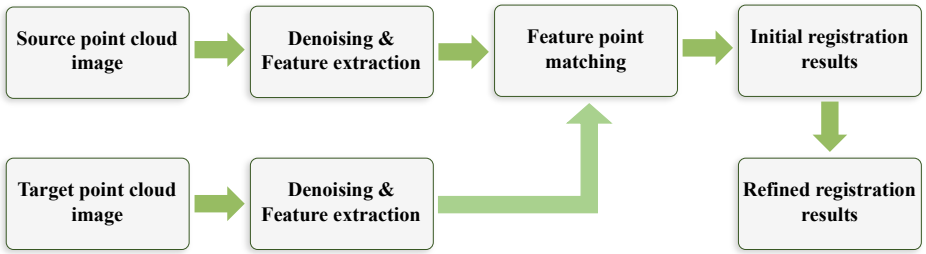


Fig. 1 – *The point cloud image registration pipeline.*

ICP has become indispensable in model construction, dimensional inspection and a great many other tasks involving range data. Every iteration begins by pairing points across the two data sets; a transformation minimizing the mean squared error (MSE) over the matched pairs is then obtained. Iteration halts once any of the termination criteria is met – the MSE drops beneath a preset threshold, the iteration budget is exhausted, or some other stopping rule fires. The method is comparatively expensive to compute, so in many settings an implementation able to run in real time, or close to it, would be valuable. Placing a metaheuristic optimization stage ahead of ICP is attractive for two reasons. The first is that ICP depends heavily on its starting alignment and will settle into a local minimum whenever the initial estimate is poor [6]. Metaheuristics, such as swarm intelligence and evolutionary computation, survey the space of transformation parameters far more globally and therefore return a more dependable initial solution. The second is that a well-designed pre-optimization step lowers the number of ICP iterations needed for convergence, which shortens computation and raises efficiency. Also, regarding to the runtime estimation of the algorithm, the metaheuristics are designed to stochastically find good solution candidate in short period of time. Maybe, it is not always an optimal solution, but it is good under defined and required system constraints.

Robustness also improves when noise, only partially overlapping clouds, or outliers are present – precisely the circumstances in which plain ICP tends to

falter. Coupling metaheuristic strategies to ICP thus sharpens alignment accuracy while simultaneously lending the computation greater stability and better scalability towards large-scale or real-time deployment.

2.2 Particle Swarm Optimization (PSO)

Particle Swarm Optimization (PSO), first introduced in [7], belongs to the family of population-based stochastic optimizers and draws its inspiration from group behaviour seen in nature, flocks of birds and schools of fish being the usual examples. It is considered as a straightforward yet capable technique for continuous optimization problems. Candidate solutions in PSO, termed particles, travel across the search space in pursuit of the optimum. A particle stands for one possible solution and is described by a position ($\boldsymbol{p}_i$) and a velocity ($\boldsymbol{v}_i$). Both the particle's own history and the knowledge accumulated by the swarm steer this motion, as expressed by (1) – (2):

$$\boldsymbol{v}_i(t+1) = \mathrm{w}\boldsymbol{v}_i(t) + \mathrm{c}_1\left(\boldsymbol{pbest}_i - \boldsymbol{p}_i(t)\right) + \mathrm{c}_2\left(\boldsymbol{gbest} - \boldsymbol{p}_i(t)\right), \tag{1}$$

$$\boldsymbol{p}_i(t+1) = \boldsymbol{p}_i(t) + \boldsymbol{v}_i(t+1). \tag{2}$$

The relation (1) also includes random coefficients drawn uniformly from [0, 1], which inject the stochastic component that lets the swarm explore the search space rather than following a fixed trajectory. Fig. 2 depicts the variables involved in the particle's movement. Velocities and positions are refreshed at every iteration by relations that weigh three contributions against one another: inertia, that is, the velocity carried over; a cognitive term reflecting the particle's own experience; and a social term reflecting what the swarm has learned. Particles are judged by fitness values returned by the model's fitness function, which is the single most important component of the algorithm. To direct subsequent movement, the best position found by each particle (***pbest***) and the best found by the swarm as a whole (***gbest***) are retained. At the start, particles are scattered randomly across the search space, and the update process is repeated either until a maximum number of iterations is reached or until the improvement in the best fitness falls below a preset threshold. Inertia weight w expresses the degree to which a particle stays committed to its previous position. Values from 0.4 to 0.9 are usual: the larger w is, the more global the search becomes, while smaller values push the search towards local behaviour. To balance these two regimes automatically, many studies employ a time-varying inertia weight that decreases over the course of the run, or a constriction factor that guarantees convergence [17]. Coefficients c_1 and c_2 weigh the cognitive (self-learning) and social (swarm-learning) contributions respectively; they normally lie between 0 and 2 and may be adjusted to suit requirements. Local search capability therefore dominates when $c_1 > c_2$, whereas global search capability dominates when $c_1 < c_2$. Despite its simplicity and fast initial convergence, PSO is known to be susceptible

to premature convergence, whereby the swarm collapses towards a local optimum before the global one is located [18].

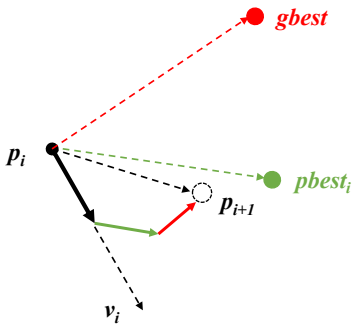


Fig. 2 – *The particle trajectory within the PSO framework.*

2.3 Differential Evolution (DE)

First proposed by Storn and Price [8] in the mid-1990s, Differential Evolution (DE) algorithm has grown into one of the most widely adopted evolutionary algorithms for real-valued optimization. It is likewise a population-based stochastic optimizer, valued for how simple it is and for how well it performs in continuous search spaces. As a global optimization tool DE has proved highly effective and has found use in fields as varied as mechanical engineering, telecommunications and pattern recognition.

More recent variants further enhance DE with adaptive control mechanisms; for instance, an adaptive DE scheme combined with a point-based strategy has been successfully applied to the challenging problem of 3D point cloud registration [9]. Several control parameters govern its behaviour decisively, notably population size (NP), crossover rate (CR), and scaling factor (F). Since these quantities regulate how exploration is traded against exploitation during the search, they bear directly on convergence speed, the quality of the solution obtained, and the stability of the algorithm.

A population of candidate solutions is maintained and progressively improved by three principal operators: mutation, crossover, and selection. Fig. 3 traces this process. Mutation forms a donor vector by selecting three distinct members of the population and adding the weighted difference between two of them (members 1 and 2) to the remaining one (member 3), as Fig. 3 shows.

Factor F fixes the weighting applied to that difference. Crossover then blends the donor vector with the target vector under the control of CR, producing a trial vector. Selection concludes the cycle: the trial vector is scored by the fitness

function and, should it outperform the target vector from which it was derived, takes the target's place in the following generation.

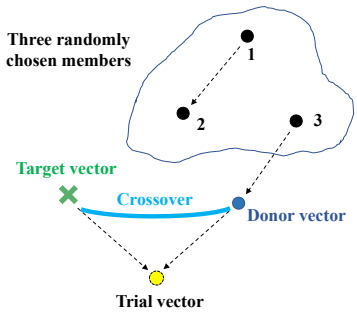


Fig. 3 –*Producing a novel candidate solution within the DE framework.*

3 Simulation

Every part of the simulation was carried out with the open-source PCL library for C++, operating on a genuine dataset produced by the authors. Photogrammetry supplied the point cloud employed here. Regarded as one of the finest non-invasive routes to 3D reconstruction, the technique is also known as *Structure from Motion*. It is revealed that vegetation contributes extra noise and irregularity to photogrammetric processing. The scene selected for the present experiment was therefore an outdoor environment dominated by trees and vegetation, chosen deliberately to make the task harder.

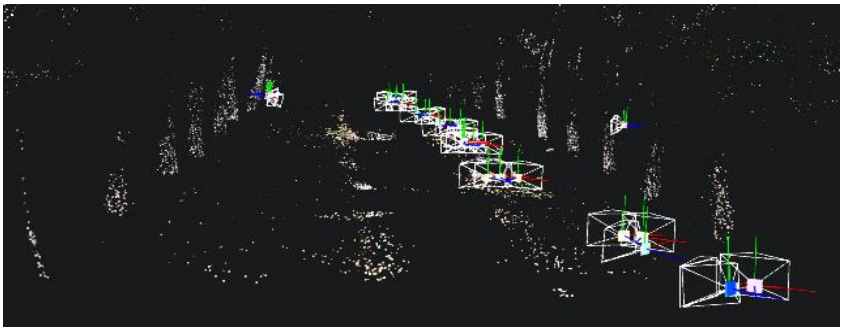


Fig. 4 – *Camera position viewpoint during the feature extraction stage of photogrammetry.*

Generally, there is two phases of 3D scene reconstruction process: data acquisition and data reconstruction. The data acquisition process was performed using Nikon D5000 camera by capturing 40-50 photographs of the chosen outdoor scene. Camera placement in this simulation followed a linear path, dictated by the linear character of the nature trail, as Fig. 4 illustrates. After

collecting all photographs, the process of data 3D reconstruction was performed according to the photogrammetry, by the Meshroom open-source software package [11] and standard Structure-from-Motion workflow. Photogrammetric reconstruction builds the 3D scene from a set of photographs taken at various angles and positions, and where the camera is placed depends on the properties of the 3D space concerned, as mentioned before.

The initial Meshroom workflow begins with image import, where the selected photographs are loaded into the software and prepared for subsequent processing. This is followed by feature extraction, during which distinctive visual characteristics, such as local patterns and edges, are detected within each image. After that, in the feature matching stage, corresponding features are identified between overlapping photographs, establishing relationships between different viewpoints, as shown in Fig. 5.



Fig. 5 – *The process of feature matching and marking descriptors.*

This matching phase is the foundation on which the entire photogrammetric reconstruction rests, since every downstream stage inherits the quality of the correspondences established between overlapping images. When features are matched accurately and densely across views, the *Structure-from-Motion* stage can recover camera poses and scene geometry with high precision, producing a well-conditioned bundle adjustment and a clean sparse point cloud that anchors the dense reconstruction. Conversely, incorrect or insufficient matches introduce outliers that propagate through the pipeline, leading to misaligned cameras, distorted or incomplete point clouds, gaps in the mesh, and visible artefacts in the final textured model. Robust matching is therefore critical not only for geometric accuracy but also for reliability, as it must remain stable under changes in viewpoint, scale, illumination, and partial occlusion that are common in real-world image sets. Finally, *Structure from Motion* uses these matched features to estimate the position and orientation of the cameras and reconstruct the spatial arrangement of the scene, resulting in a sparse 3D point cloud that forms the basis for the subsequent reconstruction stages.

Normally, the obtained point cloud should be filtered next in preparation for later processing. In this experiment, the point cloud was intentionally maintained in its raw, unprocessed state. Specifically, no statistical outlier removal or filtering techniques were applied to the data. By omitting standard pre-processing steps, the simulation was intentionally subjected to higher complexity and noise, serving as a more rigorous test of robustness for the alignment algorithm. Fig. 6 presents the vegetation-rich point cloud outdoor scene. This raw outdoor representation consists of over 200 000 points. It is used as an input cloud, which serves as the target cloud throughout the experiment. This allows the alignment algorithm to be evaluated using data that retained the natural imperfections and noise introduced during the photogrammetric reconstruction process.



Fig. 6 – *The vegetation-rich point cloud outdoor scene (kept in its raw format with over 200.000 points).*

Three principal phases constitute the simulation: transformation, downsampling, and the combined optimization-registration phase, as set out in Fig. 7. These phases represent the main steps required to prepare the input point cloud and subsequently evaluate the performance of the proposed alignment algorithm approach.

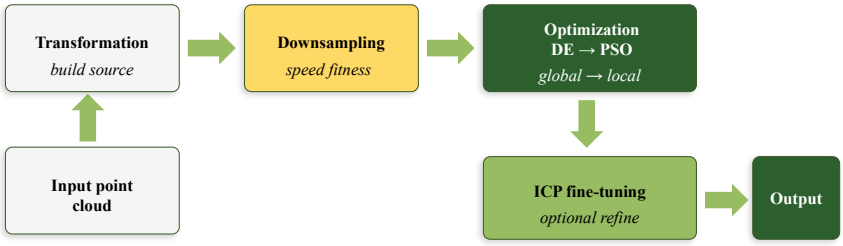


Fig. 7 – *The block diagram of the enhanced point cloud registration.*

In the transformation phase, the point cloud is subjected to a predefined spatial transformation, establishing the initial relationship between the source and target datasets. Precisely, this phase copies the target cloud and applies a 3D rotation-translation matrix to the copy, thereby creating the source cloud that must subsequently be registered against the target, as illustrated in Fig. 8. A 4×4 homogeneous transformation matrix, initialized as the identity and holding the rotation and translation components together, defined the rigid-body transformation. The source cloud was translated along the Y and Z axes and additionally rotated about the Z axis in the standard manner.

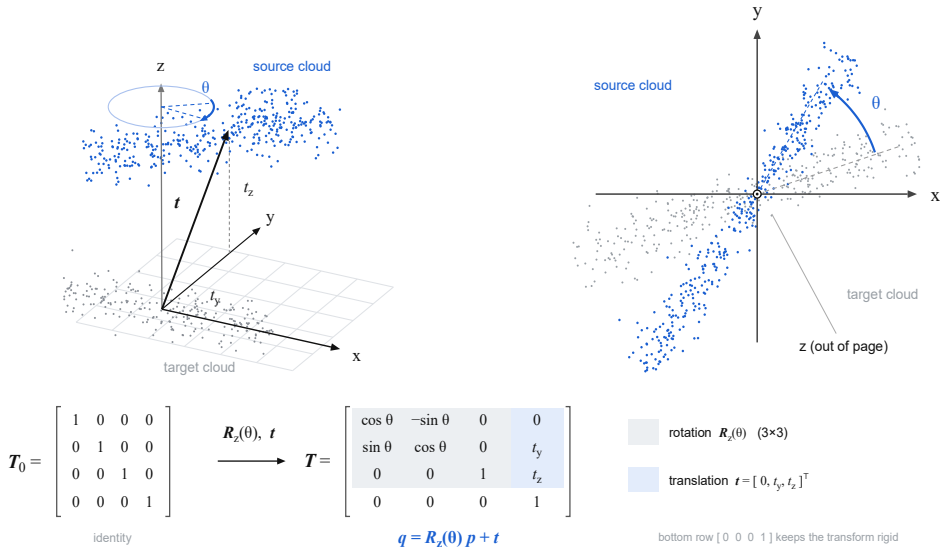


Fig. 8 – *Rigid-body transformation used to generate the source cloud from the target: rotation about Z by* θ *and translation along Y and Z, expressed as the* 4×4 *homogeneous matrix T.*

How the fitness function is specified and evaluated is decisive for any metaheuristic. A single fitness function, taken to be the RMSE (Root Mean Square Error), was adopted so that PSO and DE could be combined; it doubles as the primary metric in the experimental analysis, the second being processing time. The RMSE is computed over the Euclidean distances between corresponding source and target points, so that lower values directly reflect a tighter alignment. Point pairs are formed by matching each transformed source point to its nearest neighbour in the target cloud. All reported RMSE values are computed on the full (non-downsampled) clouds and expressed in meters. The phase that follows is thus the critical computational stage, particularly from the standpoint of the optimizers. With over 200000 points in the cloud, evaluating the fitness function and searching for nearest neighbours at every iteration can become extremely

demanding, so downsampling was used to thin the dataset [12]. Specifically, a voxel-grid filter was applied, which replaces the points within each voxel by their centroid and thus preserves the overall geometry while reducing the point count. Downsampling is confined to the metaheuristic optimization stage, where it accelerates fitness evaluation; it plays no part in the ICP registration that follows. Finally, the optimization-registration phase estimates the transformation required to align the source point cloud with the target cloud. The results obtained during these stages provide the basis for evaluating the accuracy and robustness of the registration process.

Four configurations were examined in order to analyse the proposed hybrid scheme: traditional ICP, ICP + DE, ICP + PSO and DE + PSO. So that the comparison would be meaningful, both metaheuristics were given the same population size (30) and the same iteration count (20) for the duration of the simulation. Keeping the population size and the number of iterations identical across both metaheuristics ensures that any performance difference stems from the algorithms themselves rather than from an unequal computational budget. PSO used learning coefficients c_1 and c_2 of 1.6 and an inertia weight w of 0.7, while DE used a crossover rate CR of 0.9 and a scaling factor F of 0.6. The parameters are summarized in **Table 1**.

The parameter values were adopted in line with settings commonly recommended in the literature, where empirical studies have shown them to offer a good balance between exploration and exploitation for DE [19] and PSO [20]. Deciding which algorithm should occupy the first position can be done by following the fitness function across the iterations. Fig. 9 makes it plain that PSO became trapped in a local minimum. Given its superior global exploration over wide bounds, DE was accordingly selected as the opening step of the hybrid scheme. Because the first stage of the hybrid scheme is responsible for the coarse global search over wide bounds, an algorithm with strong exploration capability is essential at this point; the refinement of the solution is then left to the subsequent stage. The search bounds were initialized marginally above the largest translation value.

Table 1

Test parameters within experimental setup.

Parameter	Value
Population size (NP)	30
Iterations	20
PSO $c_1 = c_2$	1.6
PSO inertia w	0.7
DE crossover CR	0.9
DE scaling F	0.6
Fitness metric	RMSE

The parameter values were adopted in line with settings commonly recommended in the literature, where empirical studies have shown them to offer a good balance between exploration and exploitation for DE [19] and PSO [20]. Deciding which algorithm should occupy the first position can be done by following the fitness function across the iterations. Fig. 9 makes it plain that PSO became trapped in a local minimum. Given its superior global exploration over wide bounds, DE was accordingly selected as the opening step of the hybrid scheme. Because the first stage of the hybrid scheme is responsible for the coarse global search over wide bounds, an algorithm with strong exploration capability is essential at this point; the refinement of the solution is then left to the subsequent stage. The search bounds were initialized marginally above the largest translation value.

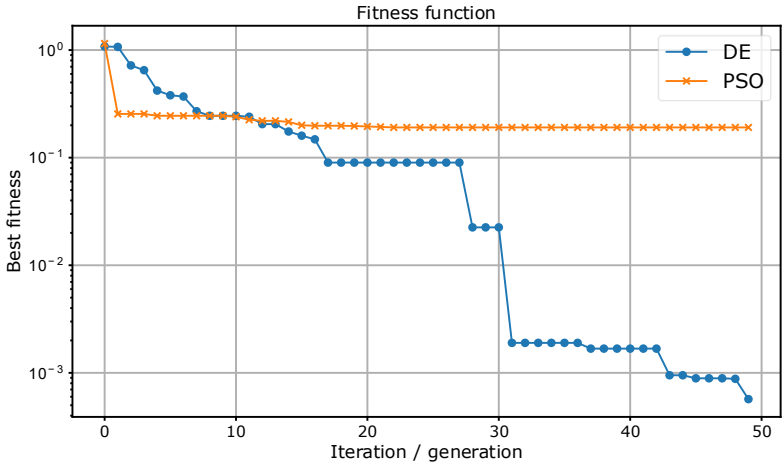


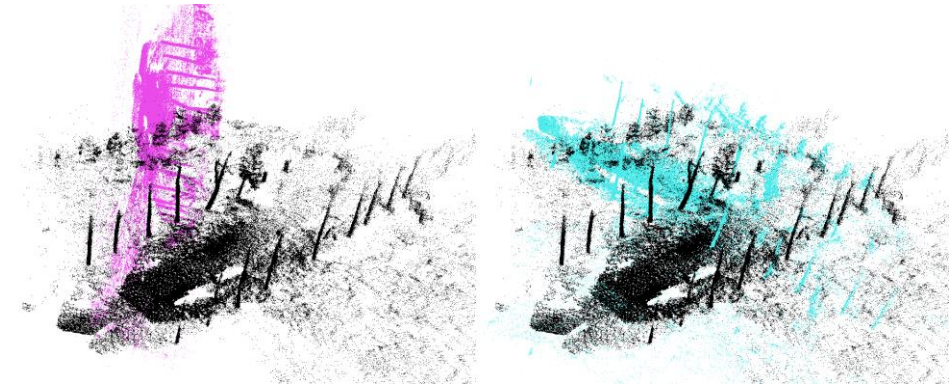
Fig. 9 – *Fitness function value for fifty performed iterations.*

4 Results

When restricted to small number of iterations without global search assistance, the standard ICP algorithm terminates prematurely before achieving stable convergence, resulting in significant misalignment due to its susceptibility to local traps. Increasing the limit of iterations allows the algorithm to run longer. Yet without global guidance, extra iterations only trap the algorithm deeper in suboptimal solutions rather than fixing the alignment, proving that simply increasing iteration counts is ineffective in noisy, complex scenes. Fig. 10 shows the alignment of the ICP algorithm without any optimization using 40 and 200 iterations. The analysis establishes that conventional ICP is not adequate for difficult registration problems.



(a)



(b)

Fig. 10 – (a) *The alignment of the ICP algorithm without any optimization using* 40 *iterations;* (b) *The alignment of the ICP without any optimization using 200 iterations.*

The metrics collected in this simulation and listed in **Table 2** show ICP settling into a local minimum by iteration 100, with the remaining iterations up to 200 producing no further gain. Quantitatively, the alignment error (RMSE) stagnated at approximately 0.181 after iteration 100, confirming that the algorithm had settled into a local minimum.

As Fig. 10 and **Table 2** make clear, the approach is computationally expensive and highly dependent on the quality of the initial pose [3]. This strong sensitivity of classical ICP to the starting alignment is a well-recognised limitation of the method [4]. For complex or real-time use, then, it ought to be optimized or exchanged for a different method which is precisely the purpose of grafting the hybrid approach onto conventional ICP.

Table 2
Performance of the conventional ICP algorithm.

Iterations	RMSE	Time [s]
40	0.2088	43.3
100	0.1824	99.4
120	0.1810	108.0
200	0.1810	192.2

As demonstrated across the different configurations, where DE combined with ICP PSO combined with ICP each offers distinct convergence profiles, integrating these metaheuristics creates a robust foundation. Ultimately, the proposed DE-PSO method leverages the synergistic strengths of both global search paradigms, delivering improved alignment performance even in unstructured, vegetation-rich outdoor environments where conventional workflows fail.

Traditional ICP relies on structural sharp edges or planar features, causing them to rapidly diverge or become trapped in local minima when processing noisy data. Blowing leaves, swaying branches, and scattered light make objects shift between scans. At the same time, thick plants block the scanner, leaving patchy ground data that tricks standard matching tools. For this reason, dealing with vegetative clutter is the trial for a point cloud registration system. If an algorithm can reliably handle the messy unpredictability of vegetation scenarios, it proves it can cope with sparse data, patchy point distributions, and unpredictable noise. The performance and visual assessments demonstrate that initializing ICP with transformation parameters pre-conditioned by population-based metaheuristics significantly speeds up convergence and enhances registration precision. By replacing arbitrary initial states and local gradient-descent constraints with a dual-stage architecture, combining dynamic global exploration with high-precision local refinement, the hybrid approach can bypass the structural traps, local minima, and sensitivity issues. Furthermore, the method provides operational flexibility by exposing customizable hyper-parameters, including population scale, convergence iteration thresholds, mutation frequency, and crossover rates. This algorithmic adaptability allows to precisely calibrate the trade-off between computational expenditure and spatial search thoroughness, tailoring the pipeline's execution to meet varying processing constraints across exceptionally diverse deployment environments.

Point cloud alignment performance and registration accuracy has been compared across distinct hybrid optimization strategies: DE combined with ICP, PSO combined with ICP, and the proposed DE-PSO method. The comparison of the three combined point cloud alignment approaches is given on Fig.11.

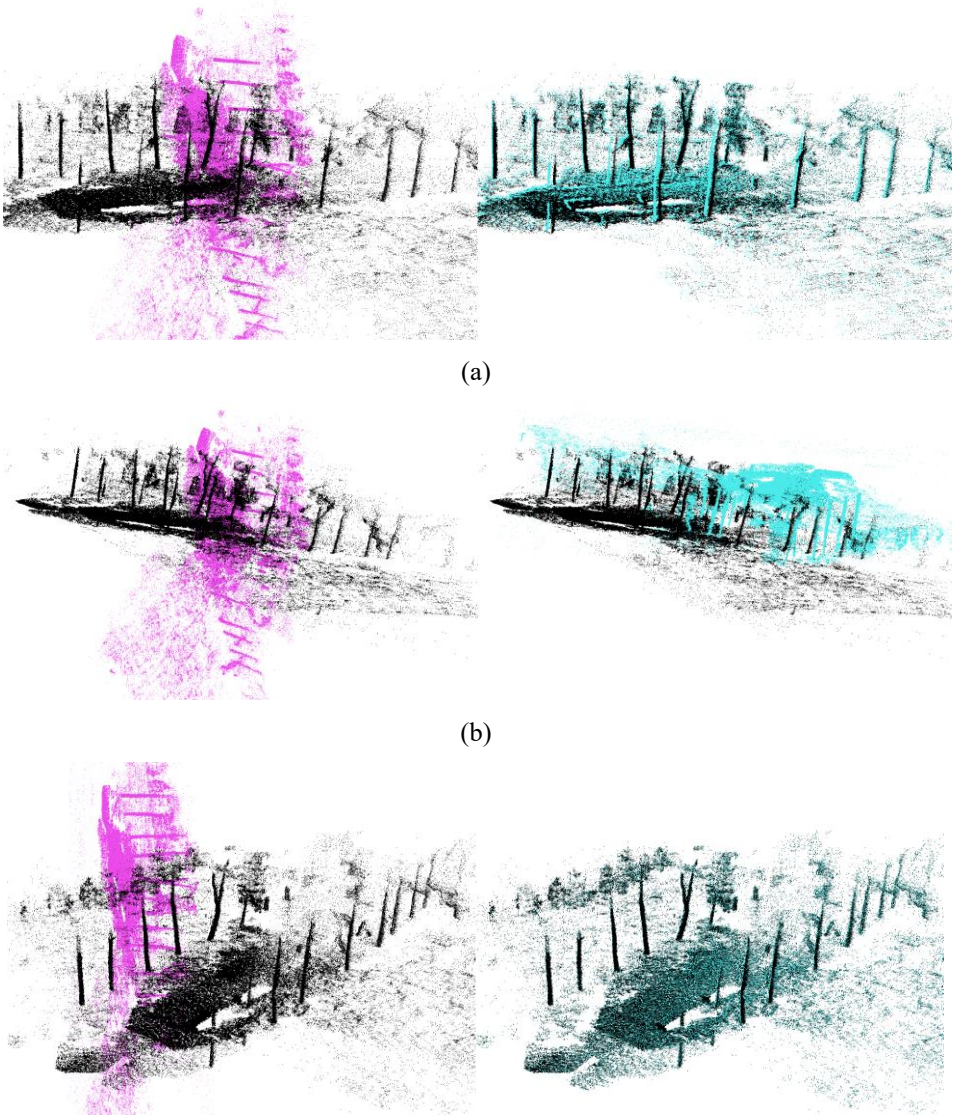


Fig. 11 – *Point cloud alignment comparisons across hybrid strategies:* (a) *DE combined with ICP, (b) PSO combined with ICP, and* (c) *the proposed DE-PSO method.*

Table 3 indicates that placing DE ahead of ICP yields more dependable results, whereas the PSO and ICP combination proved more sensitive than ICP used on its own. Best results are achieved by the DE + PSO hybrid. Its underlying idea is to let DE explore globally over a wide range and then have PSO refine the

solution locally. This ordering follows directly from the earlier observation that DE sustains stronger global exploration over wide bounds, making it the natural choice for the initial stage. Because PSO responds so sensitively to the search bounds, an adaptive arrangement was adopted: once DE finishes, the resulting RMSE is used to scale the local search bounds passed to PSO: a smaller residual error yields tighter bounds, concentrating the subsequent local search around the DE solution.

Table 3

Performance of the combined point cloud image registration algorithms.

No.	Algorithm	ICP iteration	RMSE	Runtime [s]
1	DE combined with ICP	20	0.0289	59.8
2	PSO combined with ICP	20	0.2823	44.5
3	The proposed DE-PSO	-	0.00483	44.1

DE has likewise been reported to outperform both PSO and Simulated Annealing (SA) [9]. Rather than raw RMSE, the authors of that study reported somewhat more descriptive measures. Namely, the success rate of the fitness function together with runtime. Their findings likewise suggest that DE, and still more the adaptive variant they propose, exploits space considerably more effectively and attains the smallest error.

The hybrid DE+PSO approach reaches an RMSE of approximately 0.0048, representing a 37-fold reduction compared to plain ICP under the evaluated configuration. The obtained finals errors are shown in Fig. 12, where the lowest values are shown for the proposed method.

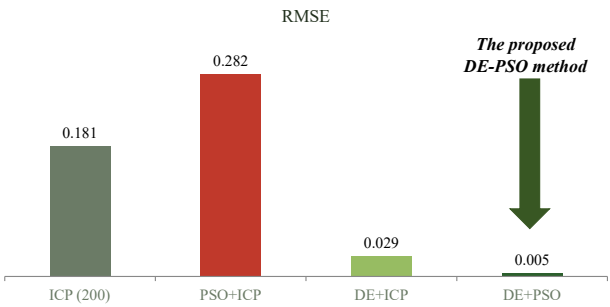


Fig. 12 – *Comparison of the point cloud image registration approaches.*

Building upon our previous work [1], this paper primarily expands the evaluation to a broader custom dataset consisting of complex vegetation point clouds to confirm the consistency and robustness of the proposed method. Vegetation-rich outdoor environments present significant processing challenges

due to severe noise, dense foliage, and irregular geometries. Hence, this work specifically focuses on such scenarios compared to alternative configurations. Although these data are inherently irregular and frequently corrupted by noise, presenting considerable difficulties during processing and interpretation, the proposed method achieves promising results across different noise levels present in the dataset.

Furthermore, to evaluate the stability of the proposed method, zero-mean Gaussian noise $N(0, \sigma^2)$ was added independently to both the source and target point clouds prior to downsampling. This synthetic perturbation simulates both sensor measurement noise and subtle random movements of foliage between scans. Because the source and target clouds are perturbed independently, exact point-to-point correspondences no longer exist, making some residual error unavoidable even under an optimal alignment. Noise levels with standard deviations from 0 to 20 mm were evaluated, and the final error was computed on the full-resolution point clouds as shown in **Table 4**. Higher noise levels were excluded because, beyond 20 mm the nearest-neighbour RMSE saturates and no longer accurately reflects the underlying noise level.

Table 4
Final registration RMSE for different Gaussian noise levels.

σ [m]	RMSE [m]
0	0.00483
0.005	0.00878
0.010	0.01014
0.015	0.01458
0.020	0.01976

The RMSE increases gradually and consistently with the noise level. From 10 mm upward, the RMSE stays approximately equal to the amount of added noise, which indicates that the remaining error is caused by the noise in the data rather than by incorrect alignment. No sudden increase in error or failure of the optimization was observed at any noise level. This shows that the method remains stable and its accuracy degrades gracefully as the noise increases. Point cloud acquisitions in unstructured environments naturally suffer from measurement noise and micro-displacements. Although DE–PSO hybrids are well suited for complex search spaces, their stability under severe spatial noise requires targeted evaluation, especially on custom vegetation point clouds.

5 Conclusion

The value of metaheuristic optimization is borne out by this study, above all for robust systems in which computation time and accuracy are both decisive.

Uniting DE, acting as the global optimizer, with local refinement by PSO gives the proposed hybrid faster convergence, lower computational cost and better alignment accuracy in demanding outdoor scenes rich in noise.

While metaheuristic optimization offers a robust and flexible framework for point cloud registration, particularly in escaping local minima and handling non-convex alignment problems without relying on large annotated datasets, the field is increasingly converging with deep learning and machine learning approaches, as proposed in [13,14]. Recent learning-based methods – such as transformer architectures and reinforcement-learning-inspired feature selection for cross-modal registration – demonstrate strong accuracy and generalization, yet they often depend heavily on training data and computational resources. Looking ahead, the future of point cloud registration likely lies in hybrid strategies that combine the global search capabilities and interpretability of metaheuristics with the powerful representational learning of deep neural networks, as proposed in [14]. Such integration promises more accurate, robust, and adaptive registration across diverse and challenging real-world conditions, reinforcing the central role of point clouds in 3D reconstruction, localization, and autonomous systems.

Future effort should extend automation so that metaheuristic parameters can be chosen to deliver high performance within a relatively short time. Systematic hyperparameter optimization and adaptive parameter tuning are the natural candidates for integration. Further experiments along these lines could examine how search bounds, population size, crossover rate, scaling factor, inertia weight and learning coefficients affect convergence, robustness and computational complexity. Work of this kind would move matters towards a fully self-adaptive metaheuristic registration framework fit for large-scale, real-time outdoor 3D reconstruction.

6 Acknowledgments

This research is supported by Ministry of Science, Technological Development and Innovation of the Republic of Serbia under contract number: 451-03-33/2026-03/200103.

7 References

[1] N. Čvorović, A. Gavrovska: Enhanced 3D Outdoor Registration Algorithm using Hybrid Metaheuristic Optimization, Proceedings of the 13th International Conference on Electrical, Electronics and Computer Engineering (IcETRAN), Silver Lake, June 2026, pp. 1 – 4.

[2] A. Mezhenin, V. Izvozchikova, A. Grigoreva, V. Shardakov: Point Cloud Registration Hybrid Method, Proceedings of the 12th Majorov International Conference on Software Engineering and Computer Systems (MICSECS), Saint Petersburg, Russia, December 2020, p. short 10.

[3] S. Rusinkiewicz, M. Levoy: Efficient Variants of the ICP Algorithm, Proceedings Third International Conference on 3-D Digital Imaging and Modeling, Quebec City, Canada, May 2001, pp. 145 – 152.

[4] T. Zinsser, J. Schmidt, H. Niemann: A Refined ICP Algorithm for Robust 3-D Correspondence Estimation, Proceedings of the International Conference on Image Processing, Barcelona, Spain, September 2003, pp. II-695.

[5] Y. Zang, C. Li, J. Tang, Z. Chen, J. Ding, S. Yang, Z. Jiang: A Composite Surface Registration Method for Freeform Surface Evaluation Based on ICP Coarse Registration and PSO Fine Registration, Optics and Lasers in Engineering, Vol. 193, October 2025, p. 109079.

[6] P. J. Besl, N. D. McKay: Method for Registration of 3-D Shapes, Proceedings of the Sensor Fusion IV: Control Paradigms and Data Structures, Boston, USA, November 1991, pp. 586-606.

[7] J. Kennedy, R. Eberhart: Particle Swarm Optimization, Proceedings of the International Conference on Neural Networks (ICNN), November 1995, pp. 1942 – 1948.

[8] R. Storn, K. Price: Differential Evolution – A Simple and Efficient Heuristic for Global Optimization over Continuous Spaces, Journal of Global Optimization, Vol. 11, No. 4, December 1997, pp. 341 – 359.

[9] T. N. Linh, T.- T. Nguyen, V.- T. Nguyen, T. Ito, T. Bui: An Adaptive Differential Evolution Algorithm with a Point-Based Approach for 3D Point Cloud Registration, Journal of Image and Graphics, Vol. 10, No. 1, March 2022, pp. 1 – 9.

[10] D. Karaboğa, Ö. Selçuk: A Simple and Global Optimization Algorithm for Engineering Problems: Differential Evolution Algorithm, Turkish Journal of Electrical Engineering and Computer Sciences, Vol. 12, No. 1, January 2004, pp. 53 – 60.

[11] C. Griwodz, S. Gasparini, L. Calvet, P. Gurdjos, F. Castan, B. Maujean, G. De Lillo, Y. Lanthony: AliceVision Meshroom: An Open-Source 3D Reconstruction Pipeline, Proceedings of the 12th ACM Multimedia Systems Conference, Istanbul, September 2021, pp. 241 – 247.

[12] E. Nezhadarya, E. Taghavi, R. Razani, B. Liu, J. Luo: Adaptive Hierarchical Down-Sampling for Point Cloud Classification, Proceedings of the IEEE/CVF Conference on Computer Vision and Pattern Recognition (CVPR), Seattle, USA, June 2020, pp. 12956 – 12964.

[13] Z. Cheng, X. Yin, J. Deng, B. Liao, Y. Chen, X. Zhou, B. Yin, T. Zhang: Adaptive Agent Selection and Interaction Network for Image-to-Point Cloud Registration, 26: Proceedings of the Fortieth AAAI Conference on Artificial Intelligence and Thirty-Eighth Conference on Innovative Applications of Artificial Intelligence and Sixteenth Symposium on Educational Advances in Artificial Intelligence (AAAI/IAAI/EAAI), Singapore EXPO, Singapore, January 2026, pp. 3335 – 3343.

[14] Y.- X. Zhang, J. Gui, B. Yu, X. Cong, X. Gong, W. Tao, D. Tao: Deep Learning-Based Point Cloud Registration: A Comprehensive Survey and Taxonomy, International Journal of Computer Vision, Vol. 134, No. 4, April 2026, p. 168.

[15] R. B. Rusu, N. Blodow, M. Beetz: Fast Point Feature Histograms (FPFH) for 3D Registration, Proceedings of the IEEE International Conference on Robotics and Automation (ICRA), Kobe, Japan, May 2009, pp. 3212 – 3217.

[16] Q.- Y. Zhou, J. Park, V. Koltun: Fast Global Registration, Proceedings of the 14th European Conference on Computer Vision (ECCV), Amsterdam, The Netherlands, October 2016, pp. 766 – 782.

[17] M. Clerc, J. Kennedy: The Particle Swarm - Explosion, Stability, and Convergence in a Multidimensional Complex Space, IEEE Transactions on Evolutionary Computation, Vol. 6, No. 1, February 2002, pp. 58 – 73.

[18] J. J. Liang, A. K. Qin, P. N. Suganthan, S. Baskar: Comprehensive Learning Particle Swarm Optimizer for Global Optimization of Multimodal Functions, IEEE Transactions on Evolutionary Computation, Vol. 10, No. 3, June 2006, pp. 281 – 295.

[19] R. Gämperle, S. D. Müller, P. Koumoutsakos: A Parameter Study for Differential Evolution, Advances in Intelligent Systems, Fuzzy Systems, Evolutionary Computation, Vol. 10, August 2002, pp. 293 – 298.

[20] M. E. H. Pedersen: Good Parameters for Particle Swarm Optimization, Hvass Laboratories Technical Report, HL1001, 2010.